Density anomaly in core-softened lattice gas

2004 J. Phys.: Condens. Matter 16 8811

(http://iopscience.iop.org/0953-8984/16/49/001)

INSTITUTE OF PHYSICS PUBLISHING JOURNAL OF PHYSICS: CONDENSED MATTER

J. Phys.: Condens. Matter **16** (2004) 8811–8822 PII: S0953-8984(04)84900-2

Density anomaly in core-softened lattice gas

Aline Lopes Balladares and Marcia C Barbosa[1]

Instituto de Física, Universidade Federal do Rio Grande do Sul, Caixa Postal 15051, 91501-970, Porto Alegre, RS, Brazil

E-mail: barbosa@if.ufrgs.br

Received 12 August 2004, in final form 7 October 2004
Published 26 November 2004
Online at stacks.iop.org/JPhysCM/16/8811
doi:10.1088/0953-8984/16/49/001

Abstract

A two dimensional lattice gas model with a 'core-softened' potential is investigated. Two liquid phases and density anomaly are found. The demixing phase transition between the two liquid phases ends at a tricritical point that is also the terminus of a critical line. The density anomaly is shown to be related to this continuous line.

1. Introduction

The phase behaviour of single component systems as particles interacting via the so-called core-softened (CS) potential has received a lot of attention recently. These potentials exhibit a repulsive core with a softening region with a shoulder or a ramp [1–4]. These models originate from the desire to construct a simple two-body isotropic potential capable of describing the complicated features of systems interacting via anisotropic potentials. This procedure generates models that are analytically and computationally tractable and that one hopes are capable of retaining the qualitative features of the real complex systems.

The physical motivation behind these studies is the recently acknowledged possibility that some single component systems display coexistence between two different liquid phases [3, 5–7]. This has opened up a discussion about the relation between the presence of two liquid phases, the existence of thermodynamic anomalies in liquids and the form of the potential. The case of water has probably been the most intensively studied. For instance, liquid water has a maximum as a function of temperature in both density and compressibility [8]. It was proposed some time ago that these anomalies might be associated with a critical point at the terminus of a liquid–liquid line, in the unstable supercooled liquid region [5], at high pressures. This hypothesis has been supported by varied experimental data [9, 10] that show that thermodynamic singularities are present in supercooled water, around 228 K and at atmospheric pressure. In spite of the limit of 235 K below which water cannot be found in the liquid phase without crystallization, two amorphous phases were observed at much lower temperatures [11].

[1] Author to whom any correspondence should be addressed.

There is evidence, although this is still under test, that these two amorphous phases are related to two liquid phases in fluid water [12, 13].

Water is not an isolated case. There are also other examples of tetrahedrally bonded molecular liquids such as phosphorus [6, 14] and amorphous silica [15] that are also good candidates for having two liquid phases. Moreover, other materials such as liquid metals [16] and graphite [17] also exhibit thermodynamic anomalies.

Acknowledging that CS potentials may engender a demixing transition between two liquids of different densities, a number of CS potentials have been proposed to model the anisotropic systems described above. The first suggestion was made many years ago by Stell and coworkers in order to explain the isostructural solid–solid transition ending in a critical point [18, 19]. Debenedetti *et al* [20], using general thermodynamic arguments, confirmed that a CS can lead to a coefficient of thermal expansion negative and consequently to density anomaly. This, together with the increase of the thermal compressibility, has been used as an indication of the presence of two liquid phases [21, 22] which may be hidden beyond the homogeneous nucleation. The difficulty with these approaches is that continuous potentials usually lead to crystallization at the region where the critical point would be expected.

In order to circumvent this problem, we study the effect of CS potentials in a lattice. Even though the lattice is not realistic, it allows us to explore the phase space in an easier way. In this work we analyse a two dimensions lattice gas with nearest-neighbour repulsive interactions and next-nearest-neighbour attraction. The system is in contact with a reservoir of temperature and particles. We show that this very simple system exhibits both density anomaly and two liquid phases. However, instead of having a critical point ending the coexistence line between the two liquid phases as one usually would expect, it has a tricritical point. The connection between the presence of criticality and the density anomaly is also shown.

The remainder of the paper goes as follows. In section 2 the model is presented and the zero temperature phases are introduced, the mean field analysis is shown in section 3, results from simulations are discussed in section 4 and our findings are summarized in section 5.

2. The model and its ground state

Our system consists of a two-dimensional square lattice with N sites. Associated to each site there is an occupational variable, σ_i. If the site is occupied by a molecule, $\sigma_i = 1$, otherwise $\sigma_i = 0$. Each site interacts with its nearest neighbours with repulsive interactions and with its next-nearest neighbours with attractive interactions (see figure 1). Therefore the Hamiltonian of this system is given by

$$H = -V_1 \sum_{\langle i,j \rangle} \sigma_i \sigma_j - V_2 \sum_{\langle\langle i,j \rangle\rangle} \sigma_i \sigma_j \tag{1}$$

where, $\langle i, j \rangle$ represents the sum over the nearest neighbours and $\langle\langle i, i \rangle\rangle$ is the sum over the next nearest neighbours. Our system is in contact with a temperature and particle reservoirs. The grand potential is given by:

$$\Phi = \langle \mathcal{H} \rangle - TS \tag{2}$$

where $\mathcal{H}$ contains the internal energy and the contribution due to the chemical potential μ, namely

$$\mathcal{H} = H - \mu \sum_{i}^{N} \sigma_i. \tag{3}$$

Let us now consider the ground state properties of this model. The Hamiltonian equation (3) allows for a number of different configurations; however, due to the lattice

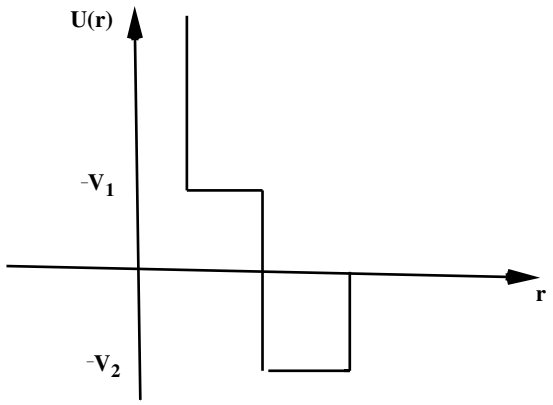

Figure 1. Schematic form of the interaction potential.

symmetry and the nature of interaction, just five of them might exhibit lower energy as the chemical potential is varied. They are (see figure 2):

- Dense liquid (dl):

$$\phi_{\mathrm{dl}} = \frac{\Phi_{\mathrm{dl}}}{N} = -2V_1 - 2V_2 - \mu. \tag{4}$$

- Uniformly diluted liquid (udl):

$$\phi_{\mathrm{udl}} = \frac{\Phi_{\mathrm{udl}}}{N} = -V_2 - \frac{1}{2}\mu. \tag{5}$$

- Structured diluted liquid (sdl):

$$\phi_{\mathrm{sdl}} = \frac{\Phi_{\mathrm{sdl}}}{N} = -\frac{1}{2}V_1 - \frac{1}{2}\mu. \tag{6}$$

- Semi-diluted liquid (semi-dl):

$$\phi_{\mathrm{semi-dl}} = \frac{\Phi_{\mathrm{semi-dl}}}{N} = -V_1 - V_2 - \frac{3}{4}\mu. \tag{7}$$

- Gas (gas):

$$\phi_{\mathrm{gas}} = \frac{\Phi_{\mathrm{gas}}}{N} = 0. \tag{8}$$

Here ϕ is the grand potential per site.

Comparing these expressions for different chemical potentials leads to the following zero temperature phase-diagram. For a positive chemical potential, $\mu \gg |V_1|$ and $\mu \gg V_2$, the lower grand potential is associated with the dense liquid phase. As the chemical potential is reduced, the interactions between molecules become relevant. The first-neighbour repulsion together with the second-neighbour attraction favours the formation of the udl phase. At $\mu = -4V_1 - 2V_2$ there is a phase transition between the dense liquid phase and the uniformly diluted liquid phase. If the chemical potential is decreased even further, at $\mu = -2V_2$ there is a transition between the uniformly diluted liquid phase and the gas phase.

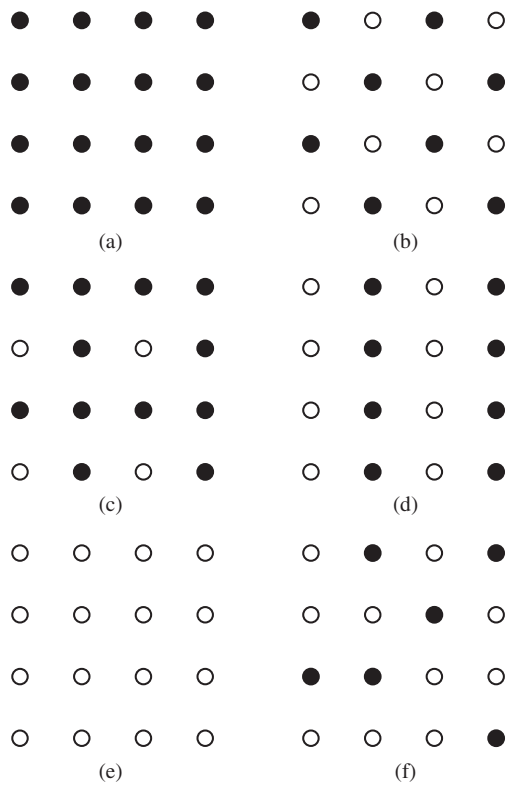

Figure 2. (a) Dense liquid phase, (b) uniformly dense liquid phase, (c) semi-diluted liquid phase, (d) structured diluted liquid phase, (e) gas phase and (f) fluid phase.

3. Mean-field

Now, let us exam the phase-diagram for nonzero temperatures employing a mean-field approximation. The symmetry of the different phases can be better visualized if the square lattice is divided into four sub-lattices as illustrated in figure 3. In this case, the density of the sub-lattice α is given by:

$$\rho_\alpha = \frac{4}{N}\sum_{j\in\alpha}\sigma_j \tag{9}$$

where the sum $j \in \alpha$ is over one of the sub-lattices $\alpha = 1, 2, 3, 4$. Note that the density of each sub-lattice varies between 0 and 1. Using the sub-lattice division, the Hamiltonian given for the equation (3) can be written as:

$$\mathcal{H} = -\sum_{\alpha=1}^{4}\sum_{i\in\alpha}\mu_\alpha^{\text{eff}}(\{\sigma_i\})\sigma_i \tag{10}$$

where

$$\mu_\alpha^{\text{eff}}(\{\sigma_i\}) = \mu_\alpha + \sum_{\beta=1}^{4}\sum_{j\in\beta}J_{ij}\sigma_j \tag{11}$$

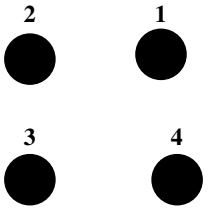

Figure 3. The sub-lattices.

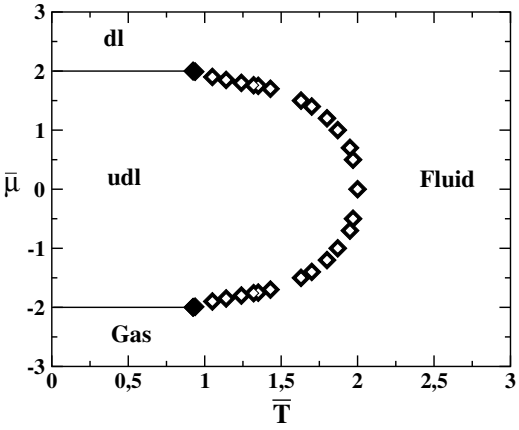

Figure 4. Phase diagram for $V_2/|V_1| = 1$. The empty diamonds are continuous lines, the solid lines are first order transitions and the filled diamonds are the tricritical points.

is the effective chemical potential acting in an ideal sub-lattice α. Here

$$\mu = \tfrac{1}{4}\sum_{\alpha=1}^{4}\mu_\alpha \tag{12}$$

is the chemical potential contribution due to the particles reservoir, while the second contribution in equation (11) is due to the interaction with other sub-lattices. The mean-field approximation we employ is to take the average of this last term, namely:

$$\bar{\mu}_\alpha^{\mathrm{eff}}(\{\sigma_i\}) = \mu_\alpha + \sum_{\beta=1}^{4}\sum_{i\in\beta} J_{ij}\langle\sigma_j\rangle = \mu_\alpha + \sum_{\beta=1}^{4}\epsilon_{\alpha\beta}\rho_\beta, \tag{13}$$

where

$$\rho_\beta = \frac{4}{N}\sum_{j\in\beta}\langle\sigma_j\rangle \tag{14}$$

is the density of the sub-lattice β and where

$$\epsilon_{\alpha\beta} = \sum_{j(\neq i)} J_{ij}, \qquad i\in\alpha, \quad j\in\beta \tag{15}$$

is an interaction parameter. The mean-field Hamiltonian then becomes

$$\mathcal{H}^{\mathrm{mf}} = -\sum_{\alpha=1}^{4}\sum_{i\in\alpha}\left(\sum_{\beta=1}^{4}\epsilon_{\alpha\beta}\rho_\beta + \mu_\alpha\right)\sigma_i - \frac{1}{2}\sum_{\alpha=1}^{4}\frac{N}{4}\sum_{\beta=1}^{4}\epsilon_{\alpha\beta}\rho_\alpha\rho_\beta \tag{16}$$

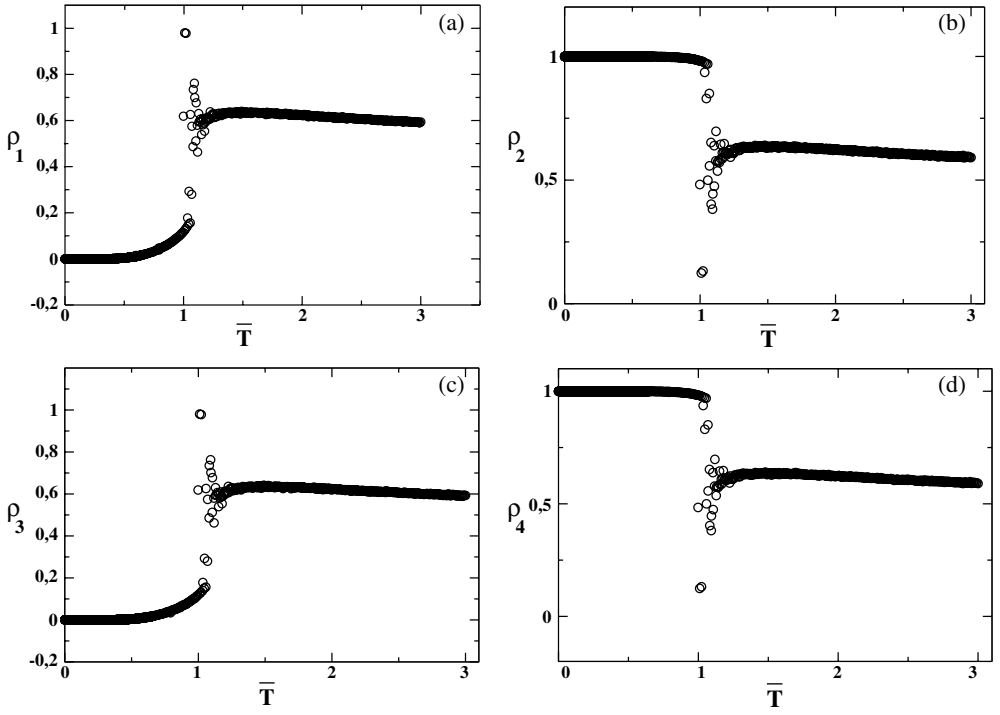

Figure 5. Densities of the (a) sub-lattice 1, (b) sub-lattice 2, (c) sub-lattice 3 and (d) sub-lattice 4 for the lattice 20×20 at $\bar{\mu} = 1.2$.

where the second term corrects for over-counting. It is straightforward to show that using equation (16) the mean field approximation for the grand potential per site is given by

$$\phi^{\mathrm{mf}} = -k_{\mathrm{B}}T \ln 2 - \frac{k_{\mathrm{B}}T}{4} \ln \cosh\left[-\frac{\beta}{2}\sum_{\beta=1}^{4}\left(\epsilon_{\alpha\beta}\rho_\beta + \mu_\alpha\right)\right] - \tfrac{1}{8}\sum_{\alpha=1}^{4}\left(\sum_{\beta=1}^{4}\epsilon_{\alpha\beta}\rho_\beta + \mu_\alpha\right) - \tfrac{1}{8}\sum_{\alpha=1}^{4}\sum_{\beta=1}^{4}\epsilon_{\alpha\beta}\rho_\alpha\rho_\beta. \tag{17}$$

The sub-lattice density can be derived both from equation (14) and from the mean field grand potential by deriving it with respect to the chemical potential, namely

$$\rho_\alpha = -4\left(\frac{\partial\phi^{\mathrm{mf}}}{\partial\mu_\alpha}\right)_{T,\mu_{\alpha\neq\beta}} \qquad \alpha = 1, \ldots, 4. \tag{18}$$

In both cases, the derivation leads to

$$\rho_\alpha = -\frac{1}{2}\tanh\left[\frac{\beta}{2}\sum_{\beta=1}^{4}(\epsilon_{\alpha\beta}\rho_\beta + \mu_\alpha)\right] - \frac{1}{2}, \qquad \alpha = 1, 2, 3, 4. \tag{19}$$

The phase-diagram, illustrated in figure 4, is obtained from solving equations (19) and (17) for different temperatures and chemical potentials. Here $V_1 = -1$ and $V_2 = 1$ are fixed. Different choices of the interaction parameters do not change the phase-diagram qualitatively. At high temperatures, all the sub-lattice densities are $\rho_\alpha = 1/2$ and the system is in the fluid phase. As the temperature is decreased at high chemical potential, $\bar{\mu} = \mu/|V_1| > 2$, the sub-lattices become full and the system goes from the fluid to the dense liquid phase. For negative

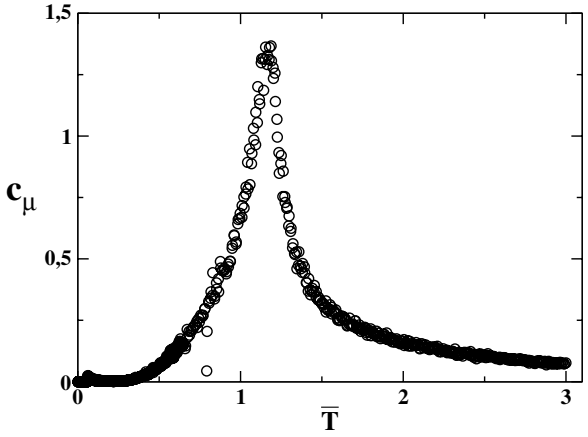

Figure 6. Specific heat for the lattice 20×20 and $\bar{\mu} = 1.2$.

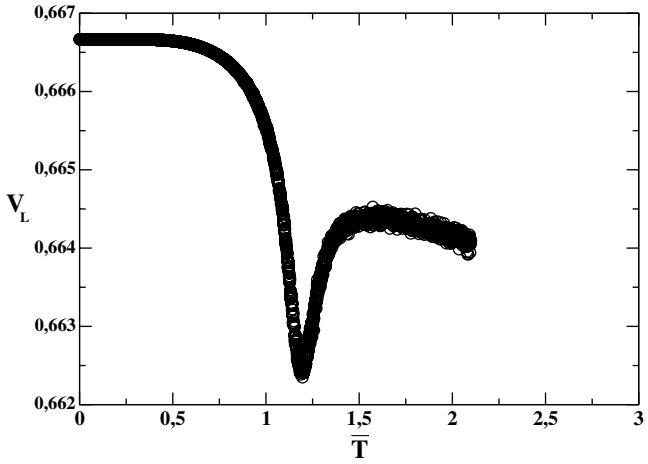

Figure 7. Fourth-order Binder's cumulant for the lattice 20×20 and for $\bar{\mu} = 1.2$.

chemical potentials, $\bar{\mu} < -2$, the sub-lattices become empty, $\rho_\alpha = 0$, and the system goes from the fluid to the gas phase. Between these two limits, $2 > \bar{\mu} > -2$, as the temperature is decreased, two opposite sub-lattices become empty while the other two get full. The system goes from the fluid phase to the udl phase through a continuous phase transition, $\bar{T}_c(\bar{\mu})$. The low temperature coexistence lines between the udl phase and the dl phase and between the udl and the gas phase are obtained by comparing the grand potentials per particle, equation (17), of these phases. The udl–dl phase boundary at $\bar{\mu} = 2$ and the udl–gas coexistence line at $\bar{\mu} = -2$ meet the critical line $T_c(\bar{\mu})$ at two tricritical points at ($\bar{T}_t = 0.924$, $\bar{\mu}_t = 2$) and ($\bar{T}_t = 0.924$, $\bar{\mu}_t = -2$), respectively.

4. Monte Carlo simulation

The rather simple mean field approach employed in the previous session is unable to account for the density anomaly. For investigating the possibility of a density anomaly in our potential,

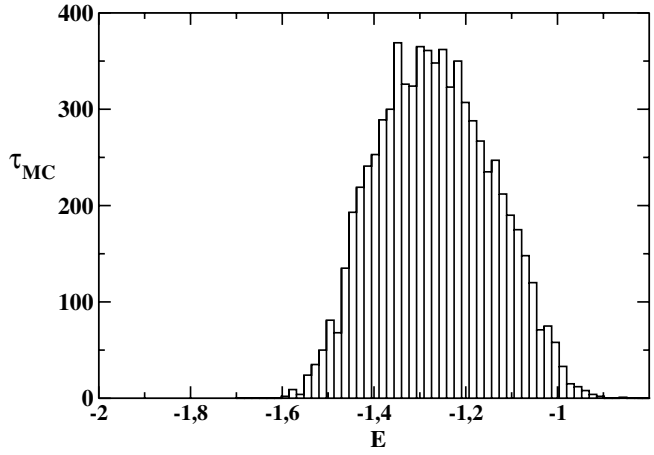

Figure 8. Energy versus Monte Carlo steps, τ_{MC} for the lattice 20×20, $\bar{\mu} = 1.2$ and $\bar{T} = 1.18$. The presence of only one peak characterizes a continuous transition.

Monte Carlo simulations in a grand canonical ensemble were performed. The Metropolis algorithm was used to study square $L \times L$ lattice and $V_2/|V_1| = 1$. Different system sizes $L = 10, 20, 30, 50$ were investigated. Equilibration time was 1000 000 Monte Carlo time steps for each lattice site.

The Monte Carlo simulations at fixed chemical potentials give the following results. At high temperatures, the density of each sub-lattice is around $\rho_\alpha = 1/2$ with sites randomly occupied in each sub-lattice, so the system is in the fluid phase. As the temperature is decreased at a fixed chemical potential, $\bar{\mu} > 2$, the density of each sub-lattice increases continuously to one. The system goes from the fluid phase to the dense liquid phase with no phase transition. If the system is cooled from the fluid phase at low chemical potential, $\bar{\mu} < -2$, the density decreases continuously from the fluid phase to the gas phase with no phase transition. As the temperature is decreased at fixed chemical potential, $-2 < \bar{\mu} < 2$, one finds that two opposite sub-lattices (1 and 3 for example) become full, while the other two sub-lattices (2 and 4) become empty, which characterizes the udl phase. Figure 5 shows that at $\bar{\mu} = 1.2$ the density of each sub-lattice jumps from the fluid phase value to the udl phase value at the critical temperature $\bar{T}_c(\bar{\mu}) \equiv T_c/|V_1| = 1.18$. Simulations for various fixed chemical potentials allow us to find the critical line $\bar{T}_c(\bar{\mu})$.

In principle, the fluctuations observed in figure 5 suggest that the transition at $\bar{T}_c(\bar{\mu})$ is continuous. This assumption is supported by the increase in the specific heat at a fixed chemical potential. Figure 6 illustrates this increase at $\bar{T}_c(\bar{\mu}) = 1.18$ for $\bar{\mu} = 1.2$.

The presence of a minimum in the fourth-order Binder cumulant given by [23]:

$$V_L = \frac{1 - \langle \mathcal{H}^4 \rangle}{3\langle \mathcal{H}^2 \rangle^2} \tag{20}$$

is an indication of criticality. Figure 7 shows V_L for $\bar{\mu} = 1.2$ obtained from our simulation. The minimum at $\bar{T}_c(\bar{\mu}) = 1.1787$ is a sign of the presence of criticality. The hypothesis that the transition at $\bar{T}_c(\bar{\mu})$ is first-order is eliminated by computing the energy histogram shown in figure 8. If the transition were first-order, two distinct peaks should be present.

In order to check the location of the coexistence lines observed by the mean-field analysis, simulations varying the chemical potential at a fixed temperature were performed. The results are shown in figure 9. For temperatures within the interval $0 < \bar{T} < 0.5$, as the chemical

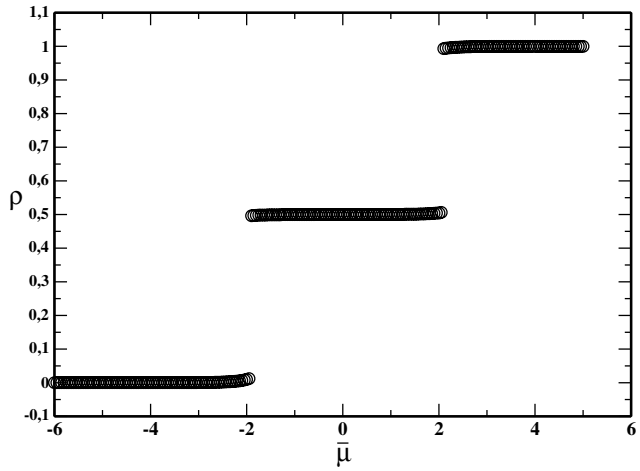

Figure 9. ρ versus $\bar{\mu}$: the first-order transitions between the gas–udl and udl–dl are illustrated.

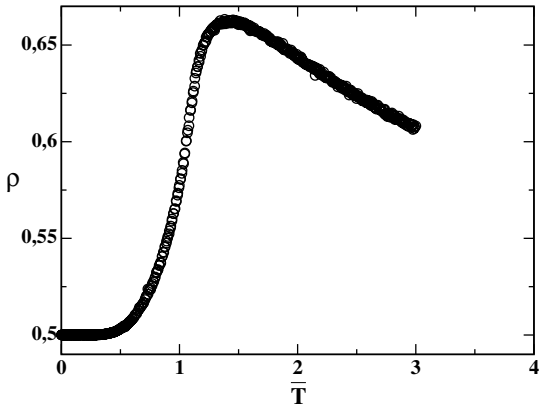

Figure 10. ρ versus T: the maximum in the density for the lattice 20×20 and $\bar{\mu} = 1.4$ is shown.

potential is increased, the system exhibits two first-order phase transitions, one between the gas and udl phase and another between the udl and the dense liquid phase.

The total density of the system at fixed chemical potential is illustrated in figure 10. Different from the mean-field result, simulations show an anomalous behaviour of the density; instead of being monotonic with temperature, the density at positive chemical potential increases as the temperature is decreased, and it has a maximum at a temperature of maximum density ($\bar{T}_{\mathrm{TMD}}(\bar{\mu})$) and then decreases. For negative chemical potentials, the complementary effect is shown in figure 11, defining a temperature of minimum density ($\bar{T}_{\mathrm{TmD}}(\bar{\mu})$).

Summarizing the results discussed above, the μ versus T phase-diagram is shown in figure 12. The critical line that separates the fluid from the uniformly diluted phase joint the phase boundaries between the uniformly diluted phase and the dense liquid and gas phases at symmetric tricritical points at ($\bar{\mu} = 2$, $\bar{T} = 0.5237$) and ($\bar{\mu} = -2$, $\bar{T} = 0.5237$), respectively. The lines of temperature of maximum density and minimum density at constant chemical potential are shown.

The p versus T phase diagram (see figure 13) is constructed by numerically integrating simulations at constant pressure. It exhibits two liquid phases, a critical line and two tricritical

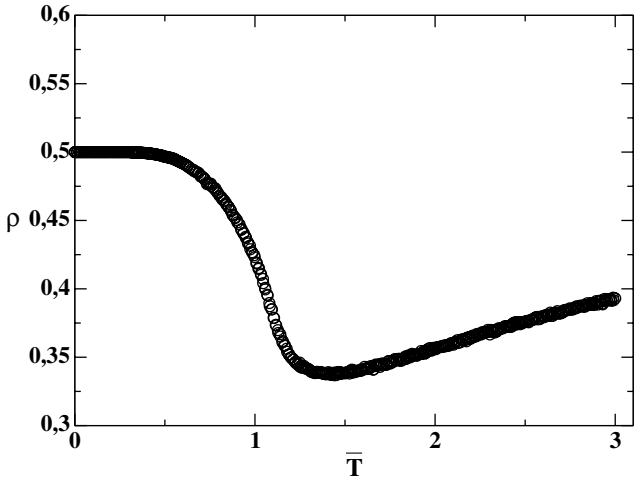

Figure 11. ρ versus T: the minimum in the density for the lattice 20×20 and chemical potential $\bar{\mu} = -1.4$ is shown.

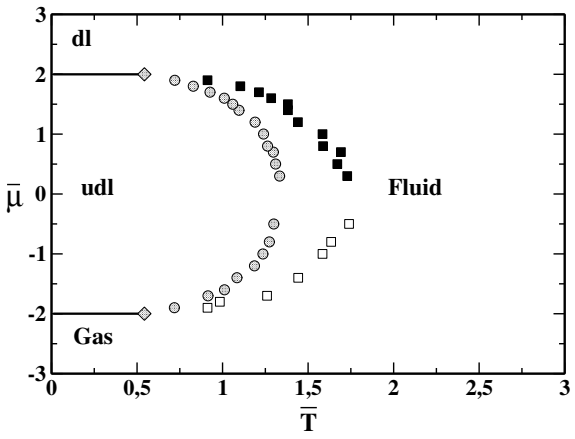

Figure 12. $\bar{\mu}$ versus $\bar{T}$ phase-diagram for the lattice 20×20. The solid lines are the first-order transitions, the circles are the critical line, the filled squares are temperatures of maximum density (TMD), the empty squares are the temperatures of minimum density (TmD) and the diamonds are the tricritical points.

points like in figure 12. Close to the critical line, there is a line of temperature of maximum density at constant pressure.

From finite size scaling analysis [24], it is possible to estimate the critical temperature of an infinite system by the following expression:

$$\bar{T}_0(\bar{\mu}) = T_c(\bar{\mu})(1 + x_0 L^{-1/2}) \tag{21}$$

where $\bar{T}_0(\bar{\mu})$ is the critical temperature of the finite system, $T_c(\bar{\mu})$ is the critical temperature of the infinite system and x_0 a parameter.

Figure 14 shows the critical temperatures of the finite systems as a function of the system size L. The value of $\bar{T}_0$ was obtained from two different methods: the maximum of the specific heat at a fixed chemical potential $\bar{\mu} = 1.7$ and the minimum of the Binder cumulant at the same chemical potential. The extrapolated critical temperatures are $\bar{T}_c(\bar{\mu}) = 0.920\,79$ and

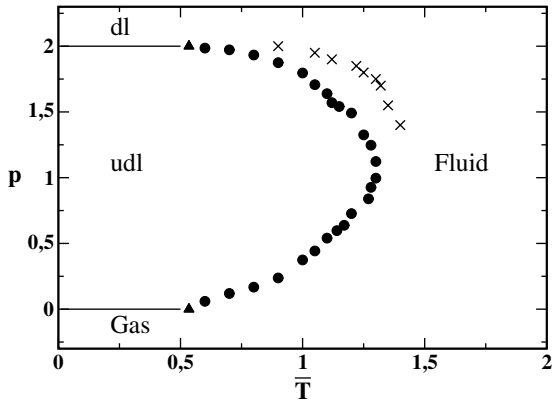

Figure 13. p versus $\bar{T}_0$ phase-diagram for the 20×20 lattice. The solid lines are first-order transitions, the filled circles are the critical line, the crosses are the TMD at constant pressure line and the filled triangles are the tricritical points.

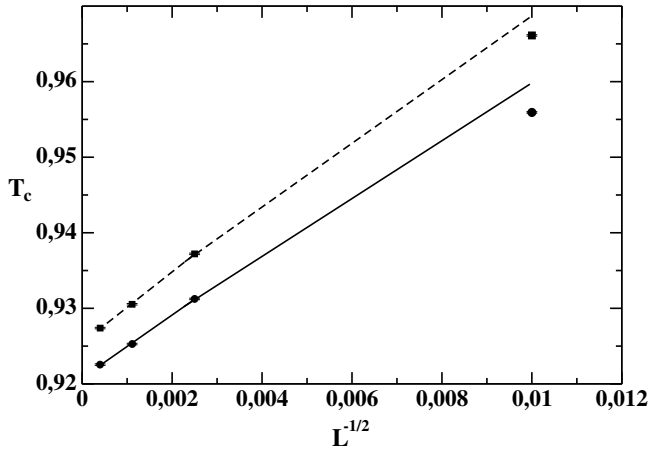

Figure 14. Minimum of the Binder cumulant (dashed line) and maximum of the specific heat (solid line) as a function of the system size $L = 10, 20, 30, 50$ for a fixed chemical potential $\bar{\mu} = 1.7$.

$\bar{T}_c(\bar{\mu}) = 0.925\,43$, respectively. The difference between these two values is within our error bars of our simulations.

5. Conclusions

In this paper the phase-diagram of a two dimensional lattice gas model with competing interactions was investigated by mean-field analysis and Monte Carlo simulations. It was shown that this system exhibits two liquid phases and a line of density anomalies.

The relation between the criticality and the density anomaly in this model goes as follows. The two liquid and the gas phases appear as a result of two competing interactions: the softened core that favours the formation of the uniformly dilute liquid phase and the chemical potential that induces the system to become completely filled or empty. For each soft-core interaction parameter, there is a limit chemical potential beyond which the system is in the dense liquid phase and another negative chemical potential beneath which the system is in the gas phase. The double criticality arises from the competition between $\bar{\mu}$ and V_1.

In systems dominated by short-range attractive forces the density increases on cooling. For the soft-core potential studied here similar behaviour is only observed when the short-range repulsion becomes irrelevant (high temperatures, $\bar{\mu} > 2$ and $\bar{\mu} < -2$). For $2 > \bar{\mu} > -2$, the soft-core repulsion prevents the density from increasing to one as the temperature is decreased. Therefore, the same competition responsible for the appearance of two liquid phases leads to the density anomaly. Similar analysis can be made when the pressure instead of the chemical potential is kept constant.

The presence of a critical line instead of a single critical point as one could generally expect [5] is not surprising. Due to the lattice structure, the udl is not one single phase but a region where two different phases coexist: alternating empty/full rows and alternating empty/full columns. These two phases become critical together with the dense liquid phase at the tricritical point that is also the locus the where critical line ends. The link between competing interactions and the presence of a density anomaly and two liquid phases is being tested in other simple models [25, 26].

Acknowledgments

This work was supported by the Brazilian science agencies CNPq, FINEP, Capes and Fapergs.

References

[1] Jagla E A 1999 *J. Chem. Phys.* **111** 8980
[2] Jagla E A 2001 *Phys. Rev.* E **63** 061509
[3] Franzese G, Malescio G, Skibinsky A, Buldyref S V and Stanley H E 2001 *Nature* **409** 692
[4] Wilding N B and Magee J E 2002 *Phys. Rev.* E **66** 031509
[5] Poole P H, Sciortino F, Essmann U and Stanley H E 1992 *Nature* **360** 324
Poole P H, Sciortino F, Essmann U and Stanley H E 1993 *Phys. Rev.* E **48** 3799
Sciortino F, Poole P H, Essmann U and Stanley H E 1997 *Phys. Rev.* E **55** 727
Harrington S, Zhang R, Poole P H, Sciortino F and Stanley H E 1997 *Phys. Rev. Lett.* **78** 2409
[6] Katayama Y, Mizutani T, Utsumi W, Shimomura O, Yamakata M and Funakoshi K 2000 *Nature* **403** 170
[7] Glosli J N and Ree F H 1999 *Phys. Rev. Lett.* **82** 4659
[8] Debenedetti P G 1996 *Metastable Liquids: Concepts and Principles* (Princeton, NJ: Princeton University Press)
[9] Mishima O and Stanley H E 1998 *Nature* **396** 329
[10] Speedy R J and Angell C A 1976 *J. Chem. Phys.* **65** 851
[11] Mishima O, Calvert L D and Whalley E 1984 *Nature* **310** 393
[12] Smith R S and Kay B D 1999 *Nature* **398** 788
[13] Mishima O and Suzuki Y 2002 *Nature* **419** 599
Martonak R, Donadio D and Parrinello M 2004 *Phys. Rev. Lett.* **92** 225702
[14] Monaco G, Falconi S, Crichton W A and Mezouar M 2003 *Phys. Rev. Lett.* **90** 255701
[15] Lacks D J 2000 *Phys. Rev. Lett.* **84** 4629
[16] Cummings P T and Stell G 1981 *Mol. Phys.* **43** 1267
[17] Togaya M 1997 *Phys. Rev. Lett.* **79** 2474
[18] Hemmer P C and Stell G 1970 *Phys. Rev. Lett.* **24** 1284
Stell G and Hemmer P C 1972 *J. Chem. Phys.* **56** 4274
[19] Hoye J S and Hemer P C 1973 *Phys. Nor.* **7** 1
[20] Debenedetti P G, Raghavan V S and Borick S S 1991 *J. Phys. Chem.* **95** 4540
[21] Sadr-Lahijany M R, Scala A, Buldyrev S V and Stanley H E 1998 *Phys. Rev. Lett.* **81** 4895
[22] Scala A, Starr F W, La Nave E, Stanley H E and Sciortino F 2000 *Phys. Rev.* E **62** 8016
[23] Challa M S S, Landau D P and Binder K 1986 *Phys. Rev.* B **34** 1841
[24] Newman M E and Barkema G T 1999 *Monte Carlo Methods in Statistical Physics* (Oxford: Clarendon)
[25] Henriques V B and Barbosa M C 2004 *Preprint* cond-mat/0407763
[26] de Oliveira A B and Barbosa M C 2004 *Preprint* cond-mat/0409138